Impact Response of Two-Layer Body Armors

A.M. Rajendran[1] and D.J. Grove[2]

Abstract: This paper presents results from a combined experimental and computational modeling study of projectile penetration response of several two – layer body armors. The projectile is a standard APM2 bullet and the target is a thin ceramic plate glued to a thick aluminum back plate. The ballistic experiments included targets with various thicknesses of both the alumina and aluminum. The projectile velocity was about 840 m/sec. Deformations and failures in various target configurations are numerically simulated using a shock wave propagation based Lagrangian finite element code (EPIC) and compared with the experimental results.

keyword: ballistic impact, microcracking, ceramic damage model, constitutive equations, shock, alumina, simulation, hydrocode.

1. Introduction

Projectile and target interaction is a complex transient problem. From the point of view of protection, the design principles for body armors include mechanisms to efficiently disperse the kinetic energy and momentum of the projectile and maintain the structural integrity of the armor after the impact. The process of absorbing the kinetic energy and momentum of a projectile can be divided into various phases: initial contact due to impact, shock propagation in the target, projectile erosion, and penetration into the armor. Energy is absorbed through plastic deformation and failure of both the target and projectile.

Traditionally, a two-layer target configuration is often employed to defeat an armor-piercing (AP) bullet. While the front layer is a polycrystalline ceramic, the back layer is a relatively soft heterogeneous glass-reinforced fiber based polymeric composite or a soft aluminum. The resistance offered by the two-layer system to projectile penetration is measured from depth of penetration (DOP) tests. In these tests, the DOP into the back-up material (thick steel or aluminum block) is measured for various ceramic plate thickness and different ceramic materials. The report by Moynihan, Chou, and Mihalcin (2000) described this "Thick Backing Technique" to evaluate three types of ceramics (alumina, silicon carbide, and boron carbide) for application in lightweight armor against a specific 0.30 caliber projectile, APM2. They presented detailed discussions on the conditions of the recovered targets.

To examine a 0.30 CAL AP projectile penetration into a thin ceramic plate backed by a metal substrate, Wilkins (1968) implemented a fracture algorithm in the Lagrangian finite-difference wave code HEMP. Wilkins modeled the evolution of the fracture conoid in thin ceramic targets by using a numerical scheme: (1) fracture initiates on a surface, (2) a maximum principal stress greater than 0.3 GPa in tension causes fracture, (3) there is a time delay for the complete fracture of a zone, (4) a fractured zone becomes a source for the fracture of a neighboring zone, and (5) fracture occurs only within a range of distance equal to or less than the time step times the crack velocity in ceramic. Under this simplistic numerical scheme, the ceramic material is assumed to obey Hooke's law; the effects of microcracking and plasticity on the degradation of stiffness and strength are not considered.

The main objective of this paper is to present results from numerical simulations of the ballistic experiments reported by Moynihan, Chou, and Mihalcin (2000). In the simulations, we employed a microcracking based three dimensional ceramic constitutive model to describe the evolution of fracture conoids and the Johnson-Cook (1985) strength model to describe all the metallic materials associated with the projectile and target. The "Background" section describes the penetration mechanisms associated with the body armor configuration. Section 3 provides details of the

---

[1] ARO, ARL, RTP, NC, USA.

[2] ARL,APG,MD,USA

geometries and materials for the APM2 projectile and the two-layer target. The computational modeling section briefly presents the ceramic constitutive model and discusses the simulation results in detail. The analyses and results are summarized in Section 5.

2. Background

A two-layered armor with a polycrystalline ceramic facing and a relatively soft heterogeneous fiber based polymeric composite as backing material has been successfully employed to defeat an armor-piercing bullet. At the initial impact, the primary defeat mechanism is to either fracture the projectile or blunt the tip of the projectile. This can be achieved through the use of a ceramic front plate whose hardness is relatively much higher than the projectile hardness. The interaction between the projectile and the armor can be analyzed by using shock wave mechanics. The impact-generated compressive shock waves that propagate into the projectile and target eventually reflect back from all the stress-free lateral surfaces to generate intense tensile stresses. Depending on the impact (striker) velocities, if the tensile stresses exceed the fracture strengths of the projectile materials, the projectile often erodes and fragments. Similarly, the ceramic plate begins to fracture due to tensile stresses at the interface of the soft substrate and ceramic. Typically, a "conoidal" fracture region develops underneath the dwelling projectile (in the ceramic layer) due to these complex wave interactions.

Based on the X-ray pictures, the projectile often dwells (penetration velocity ≈ 0) in the ceramic layer for about 15 to 20 microseconds (μs) after the initial contact. Subsequently, the residual projectile interacts with the fractured ceramic fragments. This segment of projectile could be either eroded or plastically deformed. If the ceramic layer is not thick enough to stop the projectile within its layer, then some portion of the projectile exits from the back face of the ceramic layer (with a lower velocity) into the back plate. Posttest examinations of many of the targets (rods and plates) show the presence of ring cracks, radial cracks, and fracture conoids as shown in Fig. 1. There are several types of cracks that evolve at the surface and two types of fracture fronts that evolve in the ceramic plate: 1) shear fracture in the fracture conoid region leading

to pulverization of the ceramic material, and 2) tensile fracture at the back surface of the ceramic facing due to the impedance mismatch between the ceramic facing and the soft backing plate. Accurate modeling of these macrocracks requires computationally intense algorithms such as contact, cohesive element, and adaptive mesh, as well as accurate nonlinear error estimates. Until these methods mature and become available in advanced general-purpose numerical codes, the use of conventional Lagrangian codes with some special features and reasonable constitutive models will continue to help impact design analyses involving ceramic materials.
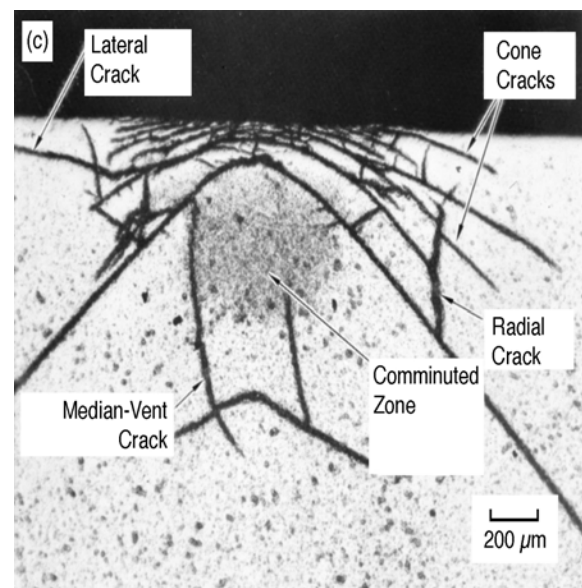

Figure 1. A variety of cracking due to a spherical projectile impact [Shockey, Marchand, et al (2002)].

When the back plate is several times thicker than that of the ceramic facing, the transient response time of the backing plate is much longer than the time required for the projectile to complete its interaction with the ceramic material. In this case, the back plate does not deform structurally, and the ceramic fragments in front of the projectile are contained, thus providing continuous resistance to projectile penetration. On the other hand, when the backing plate is thin enough to deform structurally during the period of projectile/ceramic interaction, the ceramic fragments are pushed way from the penetration cavity, and the resistance to the

projectile is reduced before the interaction or penetration is complete.

In general, the projectile defeat mechanisms involve the following: 1) Ceramic materials are weak under tensile stresses. Through tailoring the impedance match between the ceramic and the back plate, it is possible to reduce the amplitudes of rarefaction tensile waves from the interface between the ceramic face and back plate and the lateral free surfaces of the ceramic. Hence, the integrity of the ceramic material is maintained. 2) If the backup plate deformation is minimal, the comminuted and fragmented ceramic material is contained in the penetration cavity to continuously provide critical resistance to the projectile penetration.

3. Ballistic Experiments

The APM2 projectile is a jacketed, steel-cored, armor piercing round. The steel core has a Rockwell hardness of C-63 that is very effective in penetrating lightweight targets. The dimensions and components of the APM2 are shown in Fig. 2.
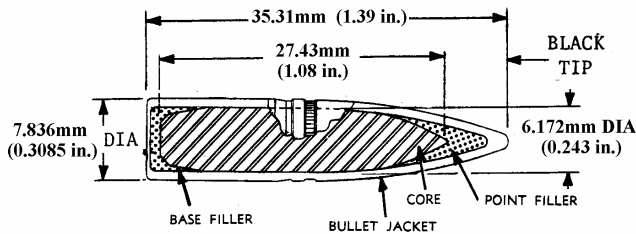

Figure 2. Caliber .30, Armor Piercing, M2.

The mass of the projectile in grains is: Jacket (Gilding Metal) 65.0, Core (Hardened Steel –Rc 63) 81.0, Point Filler (Lead) 12.0, and Base Filler (Lead) 7.7, for a total weight of 165.7 grains (10.77 grams). Note that one grain is equal to 0.065 grams. The two-layer target consisted of a hard ceramic tile in the front and a soft backup plate. The backing material was aluminum alloy 5083-H131 (Al 5083). The ceramic tile was glued to the back plate.

The APM2 projectile was launched from a caliber .306 Mann gun barrel. Projectile velocity and pitch/yaw angles were obtained by use of flash radiography. The impact velocity was maintained at 841 m/s $\pm$ 15 m/s [Moynihan, et al (2000)].

Testing was conducted on various target configurations. The first set of targets was made of various thicknesses (1.25, 2.5, 3.75, 5.0, and 6.25 mm) of ceramic facings backed by 76.2 mm thick Al 5083 blocks. Each target was prepared by adhering a ceramic tile to a 3-inch thick aluminum block using a two-part, 24-hour room temperature-cure epoxy. In comparison with the diameter and length of the projectile, the thickness of the backing material can be considered as semi-infinite in evaluating the experimental results. The experimental objective was to determine the minimum thickness of each ceramic material to defeat the projectile without any damage to the backing material (Al 5083). In other words, the projectile is completely defeated within the ceramic material layer. A thinner ceramic facing would allow the projectile to completely perforate the ceramic facing and continue penetrating into the aluminum block. The depths of penetration into the aluminum blocks (residual penetration depths) were measured using several techniques: post-test X-ray of the penetration cavity, thin rod depth gauge, and direct measurement of cut target blocks.

The second set of targets consisted of Aluminum Oxide (AL2O3-AD94) tiles (5.1 mm thick) backed by Al 5083 plates with three different thicknesses: 12.7 mm, 19.2 mm and 25.4 mm. Observations of the target responses from the second set of tests, combined with those from the first set, provide some insight on the physical and mechanical properties required to make the ceramic material more efficient in defeating this particular projectile.

Based on the first set of experiments, it was determined that the minimum thickness of Aluminum Oxide (AL2O3-AD94) required to defeat the projectile within the ceramic layer was 6.25 mm. For thinner ceramic tiles, the projectile perforated the ceramic tile and continued penetrating into the Al 5083 block. In the post-mortem examinations of the targets, no plastic deformation was found near the back surfaces of the aluminum blocks; this observation validates the assumption of semi-infinite domain with a 3-inch-thick aluminum block.

4. Computational Modeling

To simulate the various body armor configurations,

the EPIC finite element code [Johnson; Stryk; Holmquist, and Beissel (1997)] was used. EPIC is a well-established three-dimensional production code that was initially developed in the early 1970's to describe the response of solid materials to dynamic impact loading. A special feature of the 2001 version is that it includes the Generalized Particle Algorithm (GPA). When an element is eroded based on a critical plastic strain (e.g., 0.50), the eroded mass of the element is converted to a particle with the corresponding mass. These particles then continue to offer resistance to projectile penetration. Therefore, this algorithm maintains the conservation of mass, at the same time taking into account erosion and fracture. Since the GPA option enables more realistic modeling of the "dwell" phenomenon in ceramics, this option was employed in all of our simulations. Material constants required for the simulations depend on the material models used in the EPIC code. In this investigation, a ceramic model developed by Rajendran and Grove (1996, 2002) which has been implemented into the EPIC code, was used to describe the response of the AL2O3-AD94 ceramic tile.

4.1 Ceramic Constitutive Model

In the ceramic model described by Rajendran and Grove (2002), the total strain is decomposed into elastic strain (ε_{ij}^e) and plastic strain (ε_{ij}^p). The elastic strain consists of the elastic strain of the intact matrix material and the strain due to crack opening/sliding. Plastic flow is assumed to occur in the ceramic only under compressive loading when the applied pressure exceeds the pressure at the Hugoniot elastic limit (HEL). The stress-strain equations for the microcracked material are given by, $\sigma_{ij} = M_{ijkl}\varepsilon_{kl}^e$. The components of the stiffness tensor M are described by Grove and Rajendran (2002). The pressure is calculated through the Mie-Gruneisen equation of state. Microcrack damage is measured in terms of a dimensionless microcrack density γ, defined as $\gamma = N_o^* a^3$, where N_o^* is the average number of microflaws per unit volume and a, the maximum microcrack size, is treated as an internal state variable. Microcracks are assumed to extend when the stress state satisfies a generalized Griffith criterion; this criterion requires the fracture toughness K_{IC} and a dynamic friction coefficient μ as model constants. To model the effects of damage evolution during high tri-axial tensile stress loading conditions, the following stress based spall criterion was also employed in this study: microcracks initiate and grow when all three principal stresses are tensile and the maximum principal stress exceeds a critical spall threshold stress, σ_s.

The damage evolution law is derived from a fracture mechanics based relationship for a single crack propagating under dynamic loading conditions:

$$\dot{a} = n_1^{\pm} C_R \left[1 - (G_c / G_I)^{n_2^{\pm}} \right], \quad \text{where} \quad C_R \quad \text{is the}$$

Rayleigh wave speed, G_c is the critical strain energy release rate for microcrack growth, G_I is the applied strain energy release rate, and $n_1^{\pm}$ and $n_2^{\pm}$ are the model parameters that are used to limit the microcrack growth rate. The "+" superscript corresponds to microcrack opening under tension (mode I), while the "–" superscript relates to microcrack extension under compression (mode II). The crack growth rate parameters n_1^+, n_2^+, and n_2^- are always assumed to be equal to "1", but n_I^- must be calibrated for mode II crack extension. The ceramic material is assumed to pulverize under compression when the dimensionless microcrack density γ reaches a critical value of 0.75.

Effectively, the RG ceramic model requires only six constants to describe the microcracking of the intact ceramic. Based on calibration with planar plate impact data for AD995, we employed the following RG model constants for AL2O3-AD94:

$a_o = 1.5 \ \mu\text{m}, \quad N_o^* = 2 \times 10^{11} / \text{m}^3, \quad K_{IC} = 3 \ \text{MPa} \sqrt{m} ,$
$\mu = 0.60, \quad n_1^- = 0.1, \quad \text{and} \ \sigma_s = 0.5 \ \text{GPa} .$

4.2 Simulation Results

All cases simulated the projectile shown in Fig. 2 impacting a target at a velocity of 841 m/s, using EPIC's two dimensional axisymmetric geometry option. A baseline configuration was simulated wherein an APM2 projectile impacts an aluminum block without any ceramic facing. This test case was run to determine whether the code could duplicate a relatively simple impact configuration before a more complicated target configuration was introduced. The simulated DOP was 43.2 mm, as

compared to the experimental average of 46.5 mm. The relative difference was about 7.1%.

In the following simulations, we considered the target configurations with ceramic tile thicknesses of 5.1 mm for all targets. Three different backing plate thicknesses were modeled: 25.4 mm, 19.1 mm, and 12.7 mm.

For the target with a 5.1-mm alumina facing and a 25.4-mm aluminum substrate, the simulation results indicate that the projectile "dwells" for about 15 μs before it begins penetrating into the ceramic facing. Figure 3 shows the simulated damage evolution (shaded areas on the right hand side) in the ceramic plate, 10 μs after impact. A fracture conoid has formed, and the projectile's hard steel core has begun to interact with the ceramic material. In the simulation, the stripped copper jacket and lead filler continue to flow on the ceramic surface and provide some sort of confinement to the fractured ceramic. This in fact helps the ceramic to continue its resistance to projectile penetration. Then, about 15 μs after impact, the steel core begins to penetrate the pulverized ceramic material.
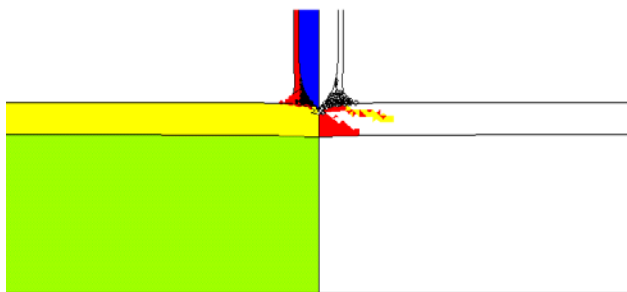

Figure 3. Simulated APM2 penetration into a 5.1-mm thick ceramic tile glued onto a 25.4-mm thick aluminum plate; t = 10 μs.

After 60 μs, the projectile has penetrated about 3.5 mm into the aluminum backing, as shown in Fig. 4. By this time, most of the jacket and filler materials have eroded away, and the penetration velocity of the partially fragmented (or eroded) steel core has dropped to zero. In the simulation, the eroded projectile and target materials were converted into particles, and the particles were ejected away from the target's free surface (see Fig. 4). The predicted DOP compared well with the test data.
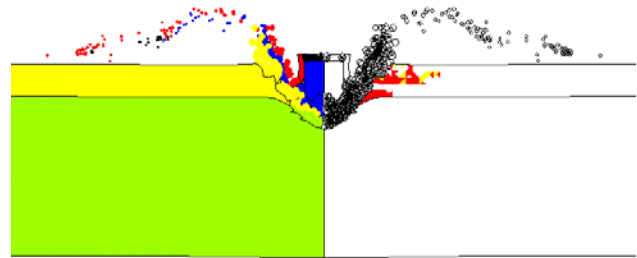

Figure 4. Simulated APM2 penetration into a 5.1-mm thick ceramic tile glued onto a 25.4-mm thick aluminum plate; t = 60 μs (final configuration).

The next simulation considered a 19.1 mm thick backup aluminum plate. The thickness of the ceramic tile was the same (5.1 mm) as in the previous simulation. Since the backup plate was thinner, the projectile was able to penetrate more easily due to the slight loss of rigidity of the back up plate. Tensile fractures occurred in the back side of the ceramic sooner compared to the configuration in which the aluminum back plate thickness was 25.4 mm. Figure 5 shows the simulated final deformed configuration of the 5.1 / 19.1 mm target at 70 μs. A slight bulging of the back side of the aluminum plate is apparent, and the residual length/mass of the projectile's steel core is about 60% greater than that of the configuration shown in Fig. 4. The simulation results were nearly identical to the experimentally observed DOP and bulge extent.
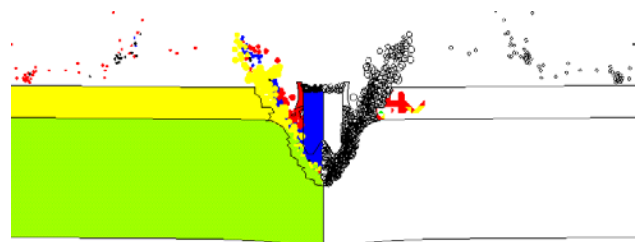

Figure 5. Simulated APM2 penetration into a 5.1-mm thick ceramic tile glued onto a 19.1-mm thick aluminum plate; t = 70 μs (final configuration).

Finally, we simulated the APM2 projectile impacting a 5.1-mm thick ceramic tile glued onto a 12.7-mm thick aluminum plate. In the experiment, the projectile penetrated into the aluminum substrate and stopped inside the plate; the aluminum plate exhibited a significant bulge at the back. The simulated final configuration also exhibited a

pronounced bulging, as can be seen in Fig. 6. As the aluminum plate deforms due to the APM2 bullet penetration, the highly-strained elements are converted to particles. The apparent crack opening on the back surface of the bulged region is a numerical artifact of the particle algorithm; the particles tend to separate in tension, even when the material is still intact. In the experiment, the severely bulged aluminum substrate did not reveal any crack patterns. In general, the simulation results compared extremely well with the experiment.
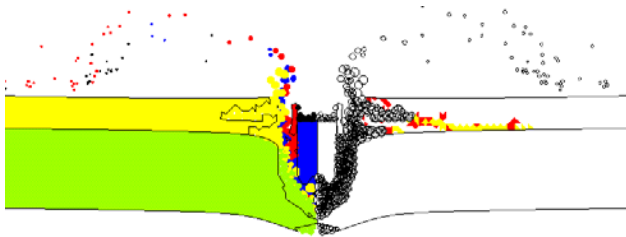

Figure 6. Simulated APM2 penetration into a 5.1-mm thick ceramic glued onto a 12.7-mm thick aluminum block; t = 80 μs (final configuration).

5. Summary

Through shock wave based finite element simulations, we demonstrated that several of the deformation and failure mechanisms that occur in a body armor configuration due to an APM2 projectile impact can be accurately modeled. The use of a microcracking based ceramic damage model in conjunction with the generalized particle algorithm to convert the eroded elements into spherical particles greatly enhanced the predictive capabilities of the EPIC code. As the thickness of the substrate was reduced, the ceramic tile's effective resistance to bullet penetration decreased. The numerical results fully support the concept of the substrate's rigidity playing an important role in defeating the bullet. Based on the modeling and simulation of a two-layer body armor configuration, it is possible to establish the critical thickness of the substrate to defeat the APM2 bullet for a given ceramic areal density.

Acknowledgements

References

Grove, D. J.; Rajendran, A.M. (2002): Overview of the Rajendran-Grove Ceramic Failure Model, in "*Ceramic Armor Materials by Design*," Eds: McCauley, Crowson, Gooch, Rajendran, Bless, Logan, Normandia, and Wax, Ceramic Transactions, Vol. 134, American Ceramic Society, pp. 371-382.

Johnson, G. R.; Cook, W. H. (1985): Fracture Characteristics of Three Metals Subjected to Various Strains, Strain Rates, Temperatures, and Pressures. *Engg. Fracture Mechanics*, Vol. 21, No. 1, pp. 31-48.

Johnson, G.R.; Stryk, R.A.; Holmquist, D.J.; Beissel, S.R. (1997) Numerical algorithms in a Lagrangian Hydrocode. Report No. WL-TR-1997-7039, Wright Laboratory, Eglin AFB, FL.

Moynihan, T.J.; Chou, S.C.; Mihalcin, A.L. (2000): Application of the Depth of Penetration Test Methodology to Characterize Ceramics for Personnel Protection, ARL-TR-2219, Army Research Laboratory, APG, MD.

Rajendran, A.M.; Grove, D.J. (1996): Modeling the Shock Response of Silicon Carbide, Boron Carbide, and Titanium Diboride, *Int. J. Impact Engng*., **Vol 18** (6) 611-631.

Rajendran, A.M.; Grove, D.J. (2002): Computational Modeling of Shock and Impact Response of Alumina, *Computer Modeling in Engineering and Sciences (CMES)*, *Int. J. Impact Engng*., **Vol 3** (3) 367-380.

Shockey, D.A.; Marchand, A.H.; Skaggs, S.R.; Cort, G.E.; Burkett, M.W.; Parker, R. (2002): Failure Phenomenology of Confined Ceramic Targets and Impacting Rods, in "*Ceramic Armor Materials by Design*," Eds: McCauley, Crowson, Gooch, Rajendran, Bless, Logan, Normandia, and Wax, Ceramic Transactions, Vol. 134, American Ceramic Society, pp. 385-402.

Wilkins, M.L. (1968): Third Progress Report of Light Armor Program, UCRL-50460, Lawrence Livermore Laboratory, Livermore, CA.